Article

# Surface Homogeneity of Anion Exchange Membranes: A Chronopotentiometric Study in the Overlimiting Current Range

Xuan Tuan Le, Pascal Viel, Dinh Phong Tran, Federico Grisotto, and Serge Palacin

## More About This Article

Additional resources and features associated with this article are available within the HTML version:

- Supporting Information
- Access to high resolution figures
- Links to articles and content related to this article
- Copyright permission to reproduce figures and/or text from this article

View the Full Text HTML

# Surface Homogeneity of Anion Exchange Membranes: A Chronopotentiometric Study in the Overlimiting Current Range

## Xuan Tuan Le,*,[†] Pascal Viel,[†] Dinh Phong Tran,[‡] Federico Grisotto,[†] and Serge Palacin[†]

*Chemistry of Surfaces and Interfaces, CEA Saclay, DSM/IRAMIS/SPCSI, F-91191, Gif-sur-Yvette Cedex, France, and Laboratoire de Chimie et Biologie des Métaux UMR 5249 (CEA-CNRS-Université J. Fourier), CEA-Grenoble iRTSV/LCBM, F- 38054 Grenoble Cedex, France*

*Received: January 7, 2009; Revised Manuscript Received: March 2, 2009*

Electrotransport of sodium chloride near and through the ASV anion exchange membrane was first investigated. Chronopotentiometric and current−voltage characteristics results have shown that the ASV membrane acts as a totally conducting plane with respect to the transport of NaCl electrolyte. SEM and AFM images contributed to confirm the overall homogeneous surface of the membrane. Further chronopotentiometric studies of the membrane were evaluated in the presence of different alkaline chloride solutions in order to explore the influence of alkali co-ions on the transport phenomena. Membrane characterization led to determine the transport number of chloride counterion in the membrane. It is reported in this work that chronopotentiometry using the Sand equation toward the homogeneous ion exchange membrane is a simple and efficient method for determination of the diffusion coefficient of the electrolytes in the bulk solution. Discussions on the transport properties of the electrolyte solutions in relation with the hydrated ion sizes allowed us to verify the diffusion coefficient of the electrolytes determined by means of chronopotentiometric method.

## 1. Introduction

Chronopotentiometry, an electrochemical method developed first by Sand,[1] allows the monitoring of changes in the electrode potential produced by a controlled current as a function of time. This technique has not only been used to evaluate kinetic effects, such as adsorption and transport phenomena near the electrode surface[2,3] and electrocatalysis performance,[4] but also applied recently to study the transport processes near and through ion exchange membranes. Taky et al.[5] used chronopotentiometric method to investigate the electrical responses and surface poisoning of a cation exchange membrane in the transfer of trivalent chromium. In the work of Wilhelm et al.,[6] chronopotentiometry was used as a tool to investigate the energy requirements of different bipolar membranes under water splitting conditions. This method is further extended in order to determine the thickness of the diffusion layer at underlimiting current density[7,8] or explain the nature of the overlimiting current.[9] More recently, chronopotentiometry has been reported to be a useful method to verify the homogeneity at the surface of ion exchange membranes.[10−12]

When an electric current is applied to a membrane in an electrolyte solution, concentration polarization phenomena arise; i.e., concentration gradients are developed in the vicinity of the membrane. The transitional process occurring near the membrane until a steady state is reached can be monitored by measuring the potential drop across the membrane as a function of time. When the electrolyte is totally depleted at the membrane surface, the potential rapidly increases. The time for this potential transition after the application of the constant current is called the transition time $\tau$. This time depends on the concentration, the diffusion coefficient of the electrolyte, and the ion transport numbers in the membrane and external solution. The relationship existing between $\tau$ and these experimental parameters are classically provided by the Sand equation by taking into consideration a linear diffusion of the electrolytes. With respect to the case of the electrodes, the Sand equation is generally used for determination of the diffusion coefficients of the electrolytes in the bulk solution.[3,13,14] Applications of this equation to the electromembrane studies are, however, somewhat contradictory. The permselectivity of the ion exchange membranes or the diffusion coefficients of the electrolytes were estimated by resorting to the Sand equation in several publications.[15−20] It has been reported too that the classical Sand equation can be modified by introducing the parameter $\varepsilon$ (the so-called effective fraction) which links to the fraction of conducting region or the pore size on the surface of electromembranes.[21,22] Such modification was applied to both types of ion exchange membranes: homogeneous and heterogeneous. Note that the heterogeneous ion exchange membranes can contain a large fraction of inert material, from 25 to 50%.[23] The purpose of this work is, therefore, to provide a better description of the application of the Sand equation to the studies of the surface homogeneity of ion exchange membranes. Although using chronopotentiometric techniques for electrode studies is sufficiently well-known, it is necessary to start from the basics of the Sand equation to understand how it applies to ion exchange membranes. In this work, the chronopotentiometric characteristics of anion exchange membranes in different alkaline chlorides are first evaluated in order to study the transport phenomenon as a function of co-ions in the solution. The observed diffusion coefficients of the electrolytes are then discussed in relation with the hydrated size of the counter- and co-ions.
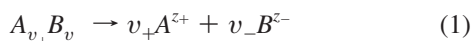
## 2. Theory

In view of the application of the chronopotentiometry technique to our system, we have to consider the case of a

---

* Corresponding author. Fax: +33 1 69 08 64 62. E-mail: xuan.tuan.le@ulb.ac.be.
† CEA Saclay, DSM/IRAMIS/SPCSI.
‡ CEA-Grenoble iRTSV/LCBM.

general electrolyte that conforms to the dissociation reaction given by

$$A_{v_+}B_{v_-} \rightarrow v_+A^{z+} + v_-B^{z-} \qquad (1)$$

In terms of the usual theory of electrochemical transport applied to the case of ion diffusion and migration, under steady-state conditions and at a constant electric current, the flux $J_j$ of one given ionic species $j$ is expressed by the Nernst−Plank equation:

$$J_j = -D_j\left\{\frac{\partial C_j(x,t)}{\partial x} + z_j C_j(x,t)\frac{F}{RT}\frac{\partial \varphi}{\partial x}\right\} \qquad (2)$$

where $D_j$ stands for the ionic diffusivity, $C_j(x,t)$ is the ionic concentration in the solution at distance $x$ from the membrane surface and at time $t$, $z_j$ is the ion electric charge number, and $\phi(x)$ is the electric potential at $x$.

According to Fick's second law of linear diffusion and with the help of eq 2, one gets

$$\frac{\partial C_j}{\partial t} = -\frac{\partial J_j}{\partial x} = D_j\frac{\partial}{\partial x}\left[\frac{\partial C_j(x,t)}{\partial x} + z_j C_j(x,t)\frac{F}{RT}\frac{\partial \varphi}{\partial x}\right] \qquad (3)$$

Otherwise, we have by definition

$$C_j(x,t) = v_j C_s(x,t) \qquad (4a)$$

$$\sum_j v_j z_j = 0 \qquad (4b)$$

Equation 3, after successive mathematical operations conforming to the condition of electroneutrality ($\sum z_j C_j(x,t) = 0$), yields the following equation:

$$\frac{\partial C_s(x,t)}{\partial t} = D_s\frac{\partial^2 C_s(x,t)}{\partial x^2} \qquad (5)$$

where the diffusion coefficient of electrolyte $D_s$ takes the form

$$\frac{1}{D_s} = \left(\frac{v_1 D_2 + v_2 D_1}{D_1 D_2}\right)\frac{1}{v_1 + v_2} \qquad (6)$$

Such definition of $D_s$ gives evidence of the phenomenon of electrostatic coupling through $\phi(x)$ of the ion diffusions.

The flux $(\bar{J}_j)$ of "$j$" in the membrane phase is a function of the applied current $i$ (mA cm$^{-2}$) and the membrane phase transport number $(\bar{t}_j)$ and is given as

$$\bar{J}_j = \frac{i\bar{t}_j}{Fz_j} \qquad (7)$$

The flux of counterion $\bar{J}_j$ within the membrane is due to migration and is equal to that in the solution $J_j$ where both migration and diffusion occur

$$J_j = \frac{it_j}{Fz_j} + v_j D_s\left(\frac{\partial C_s(x,t)}{\partial x}\right)_{x=0} \qquad (8)$$

with $t_j$ the transport number of counterion $j$ in the solution.

For applying chronopotentiometry to the membrane system, we write as follows the initial and boundary conditions necessary to solve eq 5

$$x = \infty \qquad t \geq 0 \qquad C_s(x,t) = C_0 \qquad (9)$$

$$0 \leq x \leq \infty \qquad t = 0 \qquad C_s(x,t) = C_0 \qquad (10)$$

$$x = 0 \qquad t \geq 0 \qquad \frac{\partial C_s(x,t)}{\partial x}\Big|_{x=0} = \frac{i}{v_j z_j FD_s}(\bar{t}_j - t_j) \qquad (11)$$

The solution of the second Fick equation (eq 5), as derived in the conditions given by eq 11, leads to the following variation of the electrolyte concentration $C_s(x,t)$ at the membrane surface as a function of time:

$$C_s(0,t) = C_0 - \frac{i}{z_j v_j FD_s}2(\bar{t}_j - t_j)\sqrt{\frac{D_s t}{\pi}} \qquad (12)$$

At time $\tau$, this concentration $C_s(0,t)$ reaches zero. The transition time as a function of the applied current density is readily derived from eq 12 and is given by the Sand equation written as follows:

$$\tau = \frac{\pi D_s}{4}\left(\frac{C_0 z_j v_j F}{(\bar{t}_j - t_j)}\right)^2\frac{1}{i^2} \qquad \text{(Sand equation)} \qquad (13)$$

As already indicated, $D_s$ is the diffusion coefficient of the electrolyte, $i$ the current density, $F$ the Faraday constant, $C_0$ the electrolyte concentration, and $\bar{t}_j$, $t_j$ the transport numbers of the counterion in the membrane and in the solution, respectively.

## 3. Experimental Methods

**3.1. Anion Exchange Membrane.** Some main characteristics of the ASV anion exchange membrane used in this work are presented in Table 1.

**3.2. Current−Voltage Characteristic.** Current−voltage curves were obtained using a two-compartment cell (Figure 1). This cell was composed of two compartments of equal volume (40 cm$^3$) separated by the anion exchange membrane. The apparent area of the membrane was 1.0 cm$^2$. The potential difference across the membrane was measured using two Ag/AgCl wire electrodes immersed into Luggin capillaries which were placed close to the membrane surface. The electrical current was supplied at a current scanning rate of 1 $\mu$A/s by a potentiostat/galvanostat (AutoLab, Model PGSTAT 30) connected to Ag/AgCl electrode plates.

**3.3. Chronopotentiometry.** The chronopotentiometry measurements were performed with the same two-compartment cell as shown in the section 3.2. Chronopotentiometry was carried out with a Solartron 1286 potensiostat controlled by a computer with the Corrware software. The temperature during the experiment was maintained at 25 °C.

Surface Homogeneity of Anion Exchange Membranes

*J. Phys. Chem. B, Vol. 113, No. 17, 2009* **5831**

**TABLE 1: Properties of Commercial Anion Exchange Membrane**

| name | Selemion ASV |
|---|---|
| type | homogeneous |
| fixed ionic group | $-NR_3^+$, strongly basic |
| thickness (cm)[a] | 0.011−0.015 |
| resistance ($\Omega$ cm$^2$)[a] | 2.3−3.5 |
| ion exchange capacity (mequiv/g)[b] | 3.4 (highly charged membrane) |
| transport number of Cl$^{-c}$ | >0.98 |

[a] Reference 24. [b] Reference 25. [c] Measured in this work.
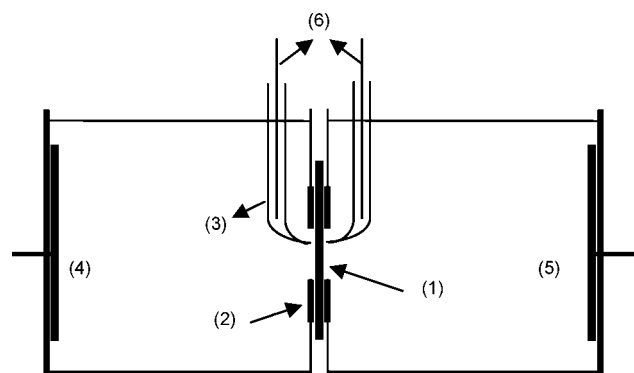
**Figure 1.** Schematic diagram of the two-compartment cell used in electrochemical measurements: (1) membrane tested; (2) rubber; (3) Luggin capillary; (4,5) electrodes (Ag/AgCl); (6) reference electrodes (Ag/AgCl wire).

**TABLE 2: Activity Coefficient of Some Alkaline Chloride Electrolytes, Reproduced from Refs 26 and 27**

| solution | 0.001 (mol/kg H$_2$O) | 0.01 (mol/kg H$_2$O) |
|---|---|---|
| LiCl | 0.976 | 0.905 |
| NaCl | 0.966 | 0.903 |
| KCl | 0.966 | 0.902 |
| CsCl | 0.965 | 0.898 |

**3.4. Transport Number of Counterion in the Membrane.** The transport number of counterion Cl$^-$ in the membranes was determined by the concentration cell method based on the diffusion potential measurements using Ag/AgCl reference electrodes.[18]

$$\varphi_m = \frac{RT}{F}\left\{(1 - 2\bar{t})\ln\left(\frac{a_2}{a_1}\right)\right\} \qquad (14)$$

where $\phi_m$ is the cell potential, $a_1$ and $a_2$ are the molal activities of MCl solutions (with M being Li$^+$, Na$^+$, K$^+$, and Cs$^+$) at the two compartments, respectively, which can be calculated from molality $m$ and activity coefficient $\gamma$ as $a = m\gamma$. In the concentration cell, we took $m_1 = 0.01$ and $m_2 = 0.001$; the corresponding values of $\gamma$ are given in Table 2. The time necessary to obtain the stationary state for the system was about 120 min. Each experiment was repeated three times, and the estimated relative error between the experimental values was below 0.4%.

**3.5. SEM and AFM Images.** The scanning electron microscopy images of the membrane sample were obtained using a FEI XL30S field emission gun scanning electron microscope (FEG-SEM). Atomic force microscopy images were recorded in the surface area of 5 $\mu$m$^2$ by Pico SPM LE (Agilent Technologies/Molecular Imaging) at the scan velocity of 0.5 $\mu$m/s.
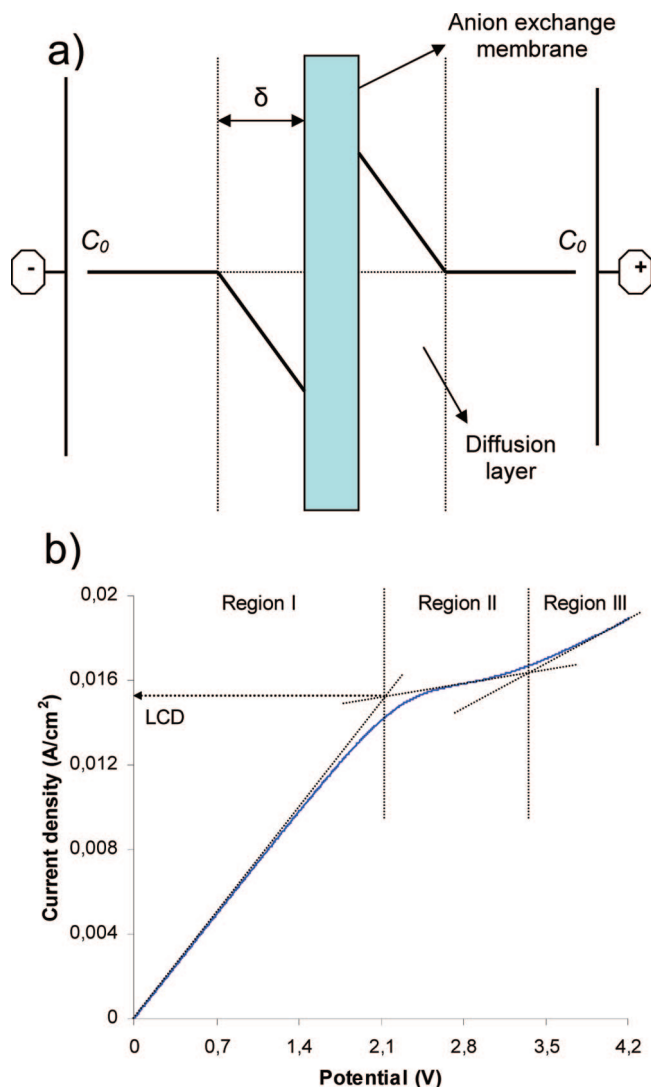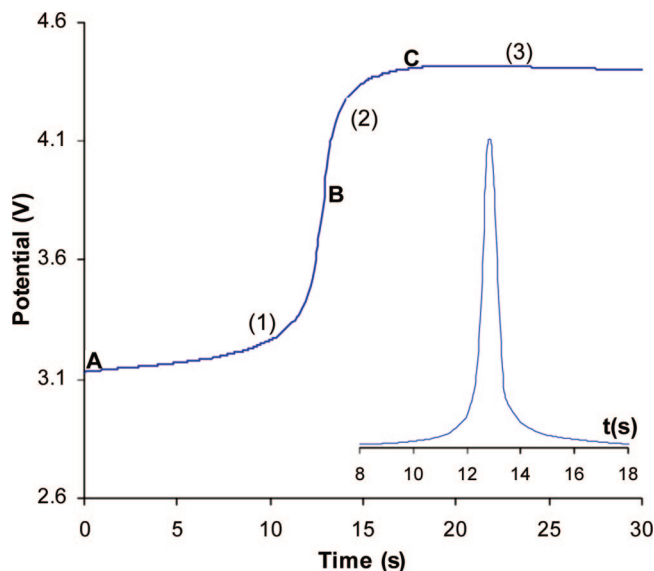


**Figure 2.** Concentration polarization for anion exchange membrane (a); current−voltage curve for the ASV membrane in contact with 0.1 M NaCl solution (b).

## 4. Results and Discussion

**4.1. Electrotransport Phenomenon of Sodium Chloride through the Membrane.** Concentration polarization phenomenon occurs at the interface between an ion exchange membrane and an electrolyte when an electrical current passes through the system due to the difference between the ion transport numbers in the electrolyte solution and in the ion exchange membrane. In the dilute compartment, the concentration becomes lower at the membrane surface than in the bulk solution, and in the concentrated compartment, at the membrane surface, concentration becomes higher. The concentration polarization generates diffusion transport and creates diffusion boundary layers at membrane surfaces (Figure 2a). The information of concentration polarization can be obtained by studying the current voltage characteristics ($I-V$ curve). Figure 2b shows typical $I-V$ curve obtained for the ASV anion exchange membrane in the presence of NaCl 0.1 M solution. Three characteristic regions were observed as expected: (I) a first region of approximately ohmic behavior transforms as voltage is increased into a second region (II), in which the current varies very little with the voltage, leading to a "plateau" corresponding to the limiting current density (LCD), followed by a third region (III) of marked current increase (overlimiting region).[28,29]

**Figure 3.** Plot of a chronopotentiometric curve of the ASV membrane and its derivative in 0.1 M NaCl solution at $i = 24$ mA/cm$^2$.



**Figure 4.** Chronopotentiometric curves of the ASV membrane in 0.1 M NaCl solution at different current densities.

According to the concentration polarization theory, the LCD value $i_{lim}$ is expressed by

$$i_{lim} = \frac{z_j v_j F D_s}{(\bar{t}_j - t_j)} \frac{C_0}{\delta} \qquad (15)$$

with $\delta$ the thickness of the diffusion layer.

Equation 15 indicates that the diffusion coefficient of the electrolyte must be known in order to determine the thickness of the diffusion layer. It is thus interesting to study the diffusion phenomena of electrolyte from the bulk solution to the membrane surface, which can be realized by chronopotentiometry, as mentioned above.

Figure 3 presents a chronopotentiometric curve of the ASV membrane in 0.1 M NaCl solution at $i = 24$ mA/cm.$^2$ The curve shown in this figure exhibits the typical shape expected for homogeneous membranes, as defined in the literature.[10–12] It is indeed observed that the value of the initial potential (point A) is due to the ohmic resistance of membrane−solution system. The first section (1) corresponds to a growth of the potential up to the inflection point (point B). It is due to the decrease in the concentration in the depleting solution near the membrane governed mainly by electrodiffusion processes. After passing the inflection point (section 2), other mechanisms of matter transfer to the membrane surface (mainly convection) become important. Note that the inflection point exists only when the current is higher than the limiting one; if the current is sufficiently small, there is no drastic passage from the electrodiffusion to another transfer mechanism. Finally, the system reaches the stationary state (point C) where the potential does no longer change with time.[10,30]

In order to apply the Sand equation to our system, we determined the transition time from the chronopotentiometric curve derivative, as suggested in several published works.[3,10,12,31] The transition time corresponds to the maximum point of the derivative curve (inset, Figure 3).

According to the Sand equation, for a given concentration and for fixed values of the diffusion coefficient of electrolyte and the transport number of counterion in solution, the transition time is a linear function of $1/i.$[2] The linear relationship in Figure
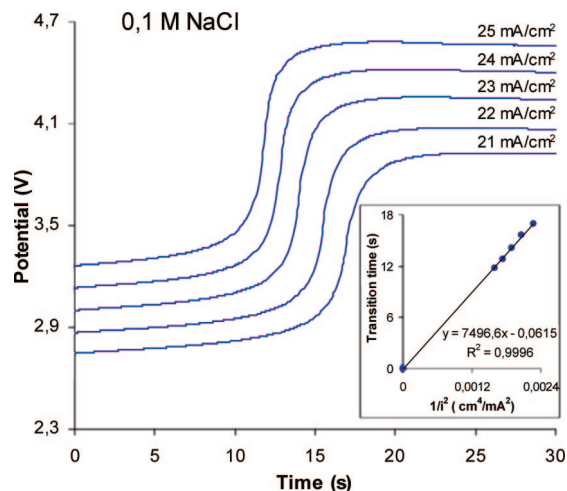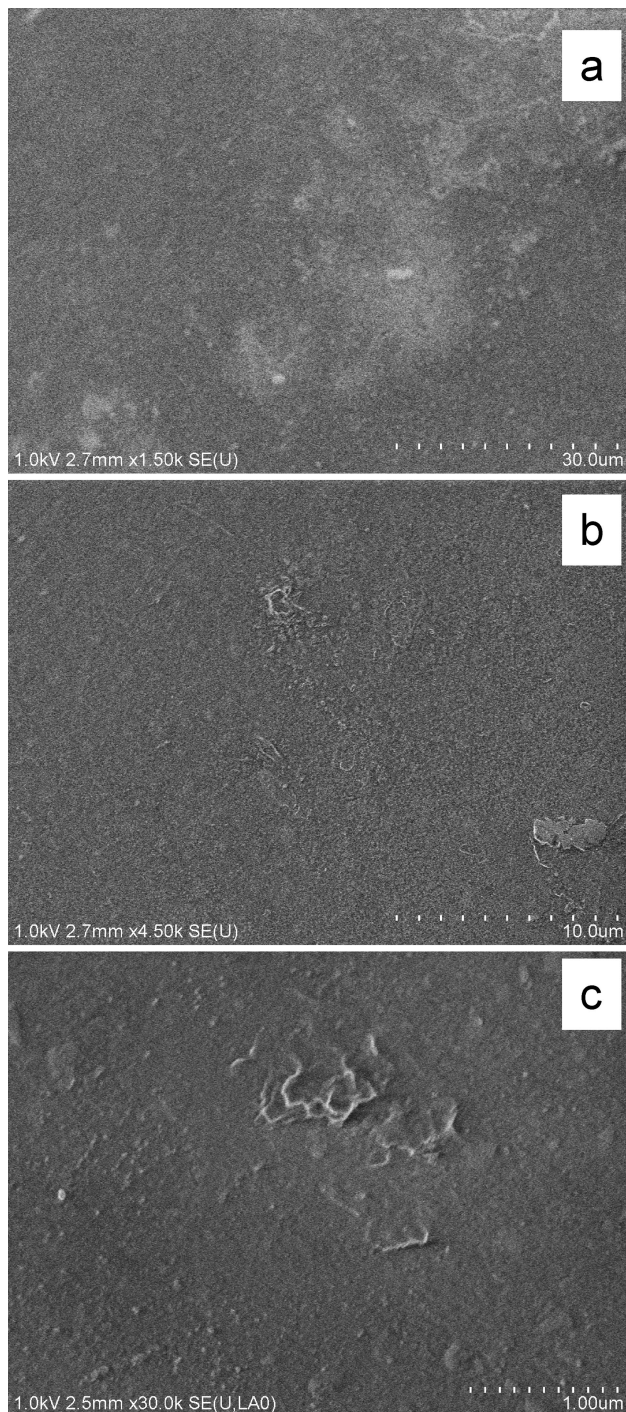
4 shows that our experimental data can be nicely described by eq 13. Note that eq 13 considers a linear diffusion (1D diffusion) of the electrolyte through the layer adjacent to the membrane and current lines normal to the surface. One can deduce that the surface of the ASV membrane is totally effective with respect to the current transport.

Homogeneous membranes consist mainly of ion exchange materials. The charged groups are more or less uniformly distributed in the membrane.[23,32] However, the surface of the membrane is not ideally homogeneous; small-sized nonhomogeneous areas exist.[11] Homogeneous membranes (such as CMS, CMV, ASV, AMX,...) are classically prepared by the paste method.[33] That method uses a small quantity of PVC in order to reinforce the physicomechanical properties of the final materials. As PVC is hydrophobic, a nonconducting region, which the ions cannot enter, appears at the surface of the resulting membranes, even the homogeneous ones. For the AMX membrane, the average dimension of those inert areas is in the range of $1-3$ $\mu$m.[11] Figure 5 presents the SEM images recorded on the surface of the ASV membrane used here at different scales. As shown here, the ASV membrane surface looks mainly homogeneous (Figure 5a) but as for AMX membranes, some micrometer-sized inert regions are also observed (Figure 5b,c). These areas are more easily observed by AFM, as shown in Figure 6. However, the size of those inert regions is quite negligible in comparison with the thickness of the diffusion layer ($50-500$ $\mu$m up to the different conditions), which explains why the Sand equation is still valid in this case. At first approximation, we can consider that the conducting fraction at the surface of homogeneous membranes equals to 100% (Figure 7a). In contrast, heterogeneous membranes are made by mixing small particles of ion exchange resins and inert binders.[23] A significant part of the surface of heterogeneous membranes is therefore impervious to ions. If the sizes of conducting and nonconducting regions are consistent with the thickness of the diffusion layer, the tangential diffusion contributes considerably to the electrochemical behavior and the problem can no longer be considered as 1D diffusion; hence the Sand equation is no longer valid. In fact, under the effect of heterogeneity, the distribution of current lines changes at the surface of the membrane. The current lines are stopped by the nonconducting region and concentrated in the conducting regions as shown in Figure 7b. The heterogeneous FT-CM membrane can be given here as a representative example. The distance between the nonconductive fibers of the
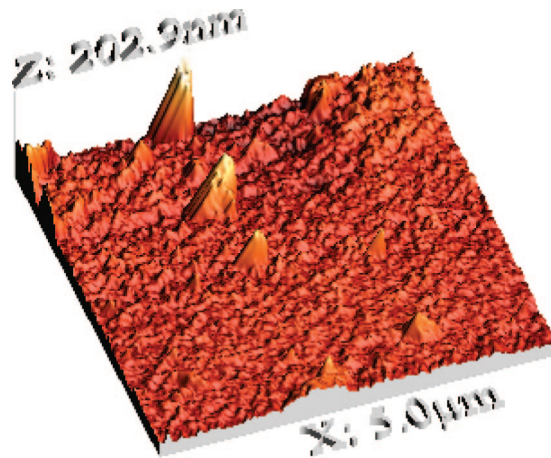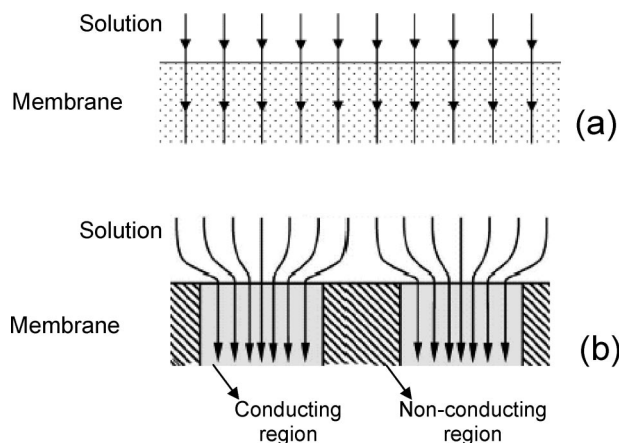
Surface Homogeneity of Anion Exchange Membranes

*J. Phys. Chem. B, Vol. 113, No. 17, 2009* **5833**



**Figure 5.** SEM images of the ASV membrane surface at different scales.



**Figure 6.** AFM image of the ASV membrane surface.



**Figure 7.** Scheme of the current line distribution close to the membrane surface: (a) homogeneous case, (b) heterogeneous case.[10,34]

membrane is greater than 200 μm, which is in the range of the boundary layer.[34]

Based on the Sand equation, the diffusion coefficient of the electrolyte in the bulk solution can be estimated if the transport numbers of counterion in the membrane and in the bulk solution are known. We get a value of 0.615 for the transport number of Cl^{−} in the bulk solution of NaCl 0.1 M.[26] The transport number of the counterion Cl^{−} in the membrane was measured as 0.991. We thus obtained a diffusion coefficient of $1.46 \times 10^{-5}$ cm²/s, which is, particularly, very close to the diffusion coefficient of NaCl 0.1 M electrolyte ($1.48 \times 10^{-5}$ cm²/s) published in literature.[26,27] By applying this value to eq 15, one

can determine the thickness of the diffusion layer: 250 μm. Such result is in good agreement with the interpretation given above.

Choi et al.[22] modified the classical Sand equation by introducing a parameter $\varepsilon$ (so-called the effective fraction) as follows:

$$i\tau^{1/2} = \frac{\varepsilon C_0 z_j v_j F}{\bar{t}_j - t_j} \frac{(\pi D)^{1/2}}{2} \qquad (16)$$

By use of this equation, the fraction of the conducting region on the surface of the CMV cation exchange membrane was found to be 95.0%, which seems to be in contradiction with the discussion above. We have shown in this work that, even when the surface contains small nonconducting regions, the membrane surface can be considered as ideally homogeneous; i.e., $\varepsilon$ approximately equals to 100%. The quasi-ideally homogeneous surface of the CMV membrane has also been confirmed in our recently published work.[12] Actually, the underestimated value of 95% given by Choi et al. can be explained easily by noting that the authors took a value of $1.99 \times 10^{-5}$ cm²/s for the diffusion coefficient of NH₄Cl (which is calculated for the infinite dilute solution) while the chronopotentiometric results were recorded in contact with 0.02 M NH₄Cl solution. The diffusion coefficient of NH₄Cl in 0.02 M solution is likely to be smaller than $1.99 \times 10^{-5}$ cm²/s (the observed behavior will be further discussed in the section 4.2). Another value for the diffusion coefficient of NH₄Cl in 0.02 M solution, $1.86 \times 10^{-5}$ cm²/s, reported by the same research group (Choi et al.[21]) looks

more reasonable. By taking this latter value, the fraction of the conducting region $\varepsilon$ on the surface of the CMV membrane can be found at 98,3%, which is very close to the expected 100%. Indeed, the modified Sand equation is not verified in this case.
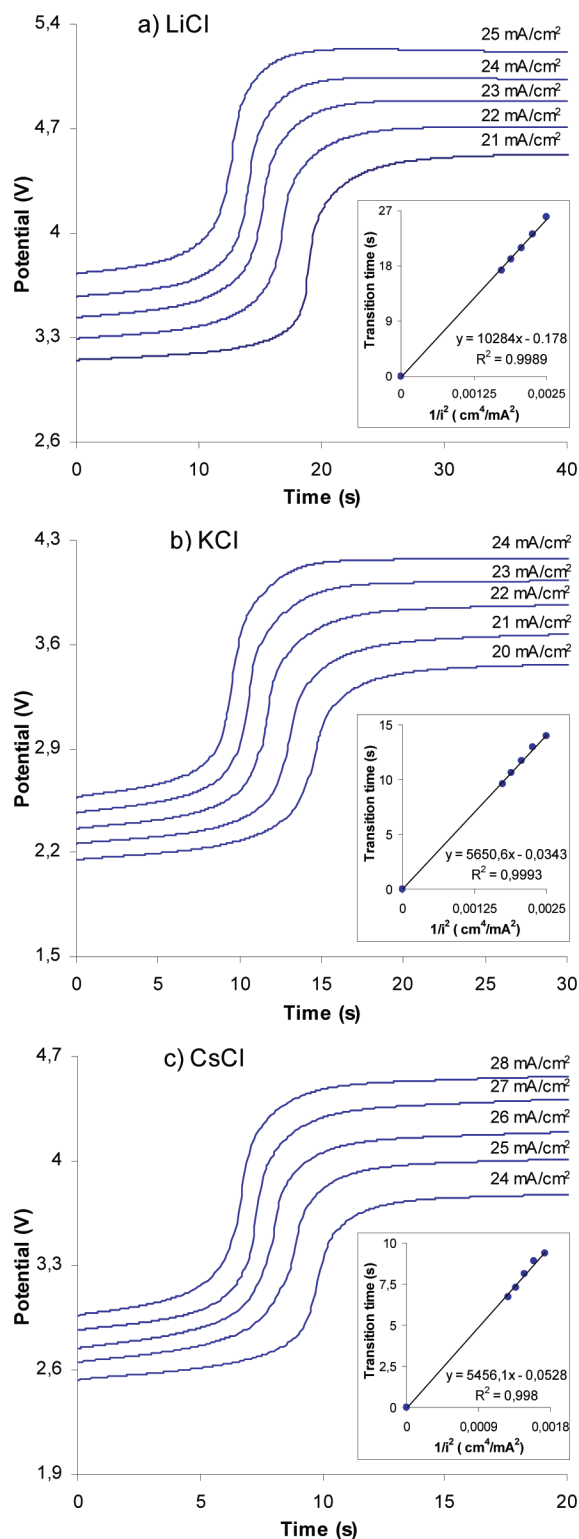
**4.2. Diffusion Coefficient of the Electrolytes and Ions in the Bulk Solutions.** It has clearly been shown that the overall surface of the ASV anion exchange membrane behaves as a conducting plane with respect to the transport of NaCl electrolyte. It might therefore be required to test the validity of the Sand equation in presence of other electrolyte solutions. Figure 8 presents the chronopotentiometric curves of the ASV membrane in contact with different alkaline electrolyte solutions. As expected, a linear relationship between the transition time and the inverse of the current density squared has been found, similarly to that obtained with NaCl solution.

Theoretical chronopotentiometric transition times depend only on mass-transfer properties. The increase in $i\tau^{1/2}$ value from LiCl, NaCl, KCl to CsCl (Table 3) accounts for the dependence of this value on electrolytes properties (such as diffusion coefficient $D_s$ and transport number of counterion in the solution $t_{Cl^-}$) and the membrane permselectivity (transport number of counterion within the membrane $\bar{t}_{Cl^-}$). Table 4 presents the transport number of counterion $Cl^-$ in the solution and in the ASV membrane.

The transport number of each ion of an electrolyte in the solution is the fraction of total current transported by this ion and is given by the ratio between its mobility and the sum of mobilities of all ions present in the solution. As a result, the transport number is linked directly to the hydrated radius of the ions (Stokes radius). Note that the hydrated radius of the co-ions studied in this work follows the sequence: $Li^+ > Na^+ > K^+ > Cs^+$ (0.239, 0.184, 0.125, and 0.119 nm, respectively[35]) which is opposite from their mobility sequence. The increase in co-ion mobilities from LiCl to CsCl solution leads to a reduction of transport number of counterion $Cl^-$ in the bulk solution. Similarly, increase in electrostatic expulsion between the co-ions and the fixed ionic groups $-NR_3^+$ inside the membrane from $Li^+$ to $Cs^+$ explains the growth of the Donnan exclusion, thus the step up in permselectivity of the ASV membrane.

From Table 4, it is also observed that the ASV membrane presents a very high permselectivity with respect to the transport of counterion $Cl^-$ in different alkaline chloride solutions (>98%). This, however, can be understood easily by noting that we have determined the transport number of chloride ion of the membrane by means of the cell concentration method in contact with the dilute solutions (0.001 and 0.01 M, respectively). Otherwise, the ASV membrane was reported as a highly charged membrane (Table 1). The quantity of co-ions in an ion exchange membrane immersed in dilute solutions ($\leq$0.1 M) is very small, in particular for the high-capacity ion exchange membrane where the Donnan exclusion becomes more effective in comparison with the low-capacity ones. A similar result has been reported in the work of Larchet et al.[36] where the transport numbers of the high charged ion exchange membranes soaked in 0.1 M solution are very close to 1, at least 0.98. Even though we did not determine the effective transport number of the ASV membrane in 0.1 M alkaline chloride solutions, our obtained transport numbers can be taken as a good approximation for treating the chronopotentiometric data.

From the Sand equation, one can evaluate the values of diffusion coefficient of the electrolytes (Table 5). It is observed that the experimental results performed with the 0.1 M solution are reasonable in comparison with the ones calculated for the



**Figure 8.** Chronopotentiometric characteristics of the ASV membrane in contact with different alkaline chloride solutions.

infinite dilute solution. Note that the medium value of the diffusion coefficient of electrolyte in the infinite dilute solution was calculated by using eq 6. Data concerning the diffusion coefficient $D_j$ of the ions are reproduced from ref 37. The difference in the two kinds of values is mainly due to the concentration of the electrolyte solution as discussed in the literature.[38] In general, the more concentrated the solution, the smaller the diffusion coefficient of the electrolyte.

Surface Homogeneity of Anion Exchange Membranes

*J. Phys. Chem. B, Vol. 113, No. 17, 2009* **5835**

**TABLE 3: Values of $i\tau^{1/2}$ Obtained with Different Electrolyte Solutions**

| electrolyte solution (0.1 M) | values of $i\tau^{1/2}$ (mA cm$^{-1}$ s$^{1/2}$) |
|---|---|
| LiCl | 100.4 |
| NaCl | 86.9 |
| KCl | 75.2 |
| CsCl | 73.8 |

**TABLE 4: Transport Number of Counterion Cl$^-$ in the Solution and in the Membrane**

| electrolyte | in the bulk solution[a] | in the membrane[b] |
|---|---|---|
| LiCl | 0.685 | 0.986 ± 0.002 |
| NaCl | 0.615 | 0.991 ± 0.003 |
| KCl | 0.509 | 0.994 ± 0.003 |
| CsCl | 0.498 | 0.998 ± 0.002 |

[a] Reference 26. [b] Determined from eq 14 by means of concentration cell method.

**TABLE 5: Diffusion Coefficient of the Studied Electrolytes in 0.1 M Solution and in Infinite Dilute Solution ($10^{-5}$ cm²/s)**

| electrolyte | determination[a] | calculation[b] |
|---|---|---|
| LiCl | 1.25 | 1.37 |
| NaCl | 1.46 | 1.61 |
| KCl | 1.82 | 1.99 |
| CsCl | 1.86 | 2.04 |

[a] Determined for 0.1 M solution. [b] Calculated for infinite dilute solution.

It has recently been remarked that the concentration dependence of transport properties (e.g., diffusion, conductivity, and viscosity) of nondiluted electrolyte solutions is still an open research subject;[39] hence, we will next treat our results in connection with the solution viscosity and conductivity.

Equation 6 applicable to our system can be rewritten as follows:

$$\frac{1}{D_{MCl}} = \frac{1}{2D_{M^+}} + \frac{1}{2D_{Cl^-}} \tag{17}$$

The diffusion coefficient of an ion $j$ in the bulk solution is related to its equivalent conductivity as the following relation:[37]

$$D_j = \frac{RT\lambda_j}{F^2|z_j|} \tag{18}$$

with $\lambda_j$ the equivalent conductivity of ion $j$ in the solution.

According to Stokes' law, the Stokes radius of an ion can be calculated with the relation

$$r_j = \frac{|z_j|eF}{6\pi\eta\lambda_j} \tag{19}$$

where $e$ is the elementary charge and $\eta$ is the solution viscosity.

From eqs 18 and 19, one deduces

$$D_{M^+} = \frac{eRT}{6\pi\eta F(r_{M^+})} \tag{20}$$

By introducing eq 20 into eq 17, we have

$$\frac{1}{D_s} = \frac{3\pi\eta F}{eRT}r_{M^+} + \frac{1}{2D_{Cl^-}} \tag{21}$$

From the literature,[38,39] it is reasonable to assume the viscosity of an electrolyte solution to be concentration dependent. In our case, all the studied electrolyte solutions have the same concentration (equal to 0.1 mol/L). At first approximation, it is considered that all alkaline chloride solutions in this work have the same viscosity. In this case, $1/D_s$ becomes a linear function of $r_{M^+}$ in accordance with eq 21.

Effectively, Figure 9 shows that the theoretical approach agrees with the experimental results. Furthermore, from the parameters in Figure 9, we can calculate the diffusion coefficient of Cl$^-$ anion. It is equal to $1.81 \times 10^{-5}$ cm²/s. The diffusion coefficient of co-ion M$^+$ may be deduced from that of chloride anion as follows:

$$D_{M^+} = \frac{D_{MCl}D_{Cl^-}}{2D_{Cl^-} - D_{MCl}} \tag{22}$$

Table 6 presents some main characteristics of the alkaline co-ions in the bulk solution of the chloride salts used in this work. As discussed in the literature,[41] the ionic radii of the alkali ions increase with increasing atomic number. The lower charge to radius ratio for the heavier ions should result in weaker hydration for the heavier ions compared to the lighter ions of the same charge. This should result in higher water activities and lower osmotic coefficients with increasing atomic number since less water is tied up by ionic hydration. Decreased cation hydration should result in increased diffusion rates since the larger (free) ions would have smaller hydrated radii. The diffusion coefficients obtained here for the alkali ions are consistent with these ideas.
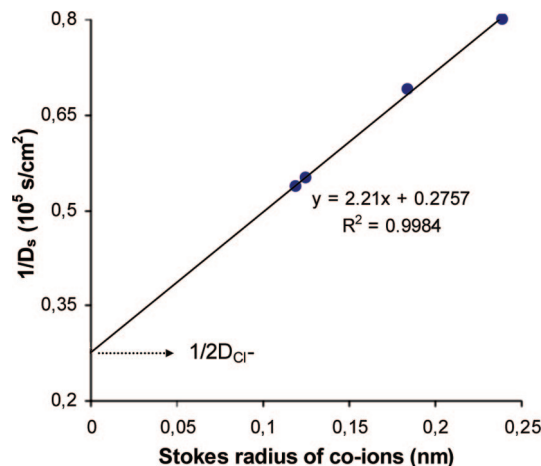


**Figure 9.** Plot of $1/D_s$ as a function of hydrated radius of the co-ions.

**TABLE 6: Main Characteristics of the Alkali Ions in 0.1 mol/L MCl Solutions**

| ion | atomic no. | ion radius (nm) | | diffusion coeff ($10^{-5}$ cm²/s)[b] |
|---|---|---|---|---|
| | | crystal[a] | Stokes | |
| Li$^+$ | 3 | 0.078 | 0.239 | 0.95 |
| Na$^+$ | 11 | 0.098 | 0.184 | 1.22 |
| K$^+$ | 19 | 0.133 | 0.125 | 1.83 |
| Cs$^+$ | 55 | 0.165 | 0.119 | 1.91 |

[a] Reproduced from ref 40. [b] Determined in this work.

## 5. Conclusion

The overall surface homogeneity of the ASV anion exchange membrane has been checked. Despite the presence of some inert regions on the surface as evidenced from SEM and AFM results, the chronopotentiometric responses of a typically homogeneous membrane have been found in the presence of different alkaline chloride solutions. As the thickness of the diffusion layer is close to 250 $\mu$m, the surface inhomogeneity of the order of several micrometers on the ASV membrane does not disturb the ion transfer, which can be described as 1D to a homogeneous surface. The Sand equation is therefore validated in that case. Such equation can be used to determine either the diffusion coefficient of the electrolytes in the bulk solution as realized in this work or the permselectivity of a homogeneous electromembrane based on the values of diffusion coefficient available in the literature. Application of the Sand equation to the case of heterogeneous membranes should take into account the size of the impermeable areas. Another important point to be underlined is that we did not observe any influence on the shape of the chronopotentiometric curves of the ASV membrane from varying co-ions in alkaline chloride salts, even though the hydrated radius of alkali co-ions affects the transport number of Cl$^-$ counterion in both the bulk solution and the membrane phase. Studies on the derived results from the Sand equation in terms of "ionic diffusion−hydration" relation in this work have shown that the use of chronopotentiometry in membrane systems can be considered within the field of electroanalytical chemistry for estimation of the electrolyte diffusion coefficients in solution.

## References and Notes

(1) Sand, H. J. S. *Philos. Mag.* **1901**, *1*, 45.

(2) Sequeira, C. A. C. *J. Electrochem. Soc.* **1989**, *136*, 2909.

(3) Bard, A. J.; Faulkner, L. R. *Electrochemical Methods, Fundamentals and Applications*, 2nd ed.; John Wiley & Sons, Inc.: New York, 2001.

(4) Gyenge, E.; Atwan, M.; Northwood, D. *J. Electrochem. Soc.* **2006**, *153*, A150.

(5) Taky, M.; Pourcelly, G.; Gavach, C.; Elmidaoui, A. *Desalination* **1996**, *105*, 219.

(6) Wilhelm, F. G.; van der Vegt, N. F. A.; Strathmann, H.; Wessling, M. *J. Membr. Sci.* **2002**, *199*, 177.

(7) Sistat, P.; Pourcelly, G. *J. Membr. Sci.* **1997**, *123*, 121.

(8) Larchet, C.; Nouri, S.; Auclair, B.; Dammak, L.; Nikonenko, V. *Adv. Colloid Interface Sci.* **2008**, *139*, 45.

(9) Ibanez, R.; Stamatialis, D. F.; Wessling, M. *J. Membr. Sci.* **2004**, *239*, 119.

(10) Pismenskaia, N.; Sistat, P.; Huguet, P.; Nikonenko, V.; Pourcelly, G. *J. Membr. Sci.* **2004**, *228*, 65.

(11) Volodina, E.; Pismenskaya, N.; Nikonenko, V.; Larchet, C.; Poucelly, G. *J. Colloid. Interface Sci.* **2005**, *285*, 247.

(12) Xuan Tuan, L.; Verbanck, M.; Buess-Herman, C.; Hurwitz, H. D. *J. Membr. Sci.* **2006**, *284*, 67.

(13) Chao, M. S. *J. Electrochem. Soc.* **1968**, *115*, 1172.

(14) Bermejo, M. R.; Gomez, J.; Martinez, A. M.; Barrado, E.; Castrillejo, Y. *Electrochim. Acta* **2008**, *53*, 5106.

(15) Ramachandraiah, G.; Ray, P. *J. Phys. Chem. B* **1997**, *101*, 7892.

(16) Vyas, P. V.; Ray, P.; Adhikary, S. K.; Shah, B. G.; Rangarajan, R. *J. Colloid Interface Sci.* **2003**, *257*, 127.

(17) Nagarale, R. K.; Shahi, V. K.; Thampy, S. K.; Rangarajan, R. *React. Funct. Polym.* **2004**, *61*, 131.

(18) Xuan Tuan, L. *J. Colloid Interface Sci.* **2008**, *325*, 215.

(19) Kontturi, K.; Mafe, S.; Manzanares, J. A.; Murtomäki, L.; Viinikka, P. *Electrochim. Acta* **1994**, *39*, 883.

(20) Kontturi, K.; Mafe, S.; Manzanares, J. A.; Sundholm, G.; Vapola, R. *Electrochim. Acta* **1996**, *42*, 2569.

(21) Choi, J. H.; Moon, S. H. *J. Membr. Sci.* **2001**, *191*, 225.

(22) Choi, J. H.; Kim, S. H.; Moon, S. H. *J. Colloid Interface Sci.* **2001**, *241*, 120.

(23) Helfferich, F. *Ion exchange*; McGraw-Hill Book Co.: New York, 1962.

(24) Xu, T. *J. Membr. Sci.* **2005**, *263*, 1.

(25) Toshikatsu, H. US Patent 5376250, 1994.

(26) Lobo, V. M. M.; Quaresma, J. L. *Handbook of electrolyte solutions*; Elsevier: New York, 1989.

(27) Robinson, R. A.; Stokes, R. H. *Electrolyte Solutions*, 2nd ed.; Butterworths Scientific Publications: London, 1959.

(28) Chamoulaud, G.; Belanger, D. *J. Colloid Interface Sci.* **2005**, *281*, 179.

(29) Manzanares, J. A.; Murphy, W. D.; Mafe, S.; Reiss, H. *J. Phys. Chem.* **1993**, *97*, 8524.

(30) Belova, E. I.; Lopatkova, G. Y.; Pismenskaia, N. D.; Nikonenko, V. V.; Larchet, C.; Pourcelly, G. *J. Phys. Chem. B* **2006**, *110*, 13458.

(31) Sturrock, P. E.; Hughey, J. L.; Vaudreuil, B.; O'Brien, G. E.; Gibson, R. H. *J. Electrochem. Soc.* **1975**, *122*, 1195.

(32) Sata, T. *J. Membr. Sci.* **2000**, *167*, 1.

(33) Mizutani, Y. *J. Membr. Sci.* **1990**, *49*, 121.

(34) Balster, J.; Yildirim, M. H.; Stamatialis, D. F.; Ibanez, R.; Lammertink, R. G. H.; Jordan, V.; Wessling, M. *J. Phys. Chem. B* **2007**, *111*, 2152.

(35) Pyrasch, M.; Toutianoush, A.; Jin, W.; Schnepf, J.; Tieke, B. *Chem. Mater.* **2003**, *15*, 245.

(36) Larchet, C.; Dammak, L.; Auclair, B.; Parchikov, S.; Nikonenko, V. *New J. Chem.* **2004**, *10*, 1260.

(37) Lide D. R. *Handbook of Chemistry and Physics*, 80th ed.; CRC Press: Boca Raton, FL, 1999−2000.

(38) Jenkins, B.; Donald, H.; Marcus, Y. *Chem. Rev.* **1995**, *95*, 2695.

(39) Esteves, M. J. C.; Cardoso, M. J. E. de M.; Barcia, O. E. *Ind. Eng. Chem. Res.* **2001**, *40*, 5021.

(40) Pau, P. C. F.; Berg, J. O.; McMillan, W. G. *J. Phys. Chem.* **1990**, *94*, 2671.

(41) Rard, J. A.; Miller, D. G. *J. Chem. Eng. Data* **1980**, *25*, 211.